Monolithic Integration in InGaAs–InGaAsP Multiple-Quantum-Well Structures Using Laser Intermixing

Andrew McKee, C. J. McLean, Giuseppe Lullo, A. Catrina Bryce, Richard M. De La Rue, John H. Marsh, *Senior Member, IEEE,* and Christopher C. Button

Abstract— **The bandgap of InGaAs–InGaAsP multiple-quantum-well (MQW) material can be accurately tuned by photoabsorption-induced disordering (PAID), using a Nd:YAG laser, to allow lasers, modulators, and passive waveguides to be fabricated from a standard MQW structure. The process relies on optical absorption in the active region of the MQW to produce sufficient heat to cause interdiffusion between the wells and barriers. Bandgap shifts larger than 100 meV are obtainable using laser power densities of around 5 W · mm^{-2} and periods of illumination of a few minutes to tens of minutes. This process provides an effective way of altering the emission wavelengths of lasers fabricated from a single epitaxial wafer. Blue shifts of up to 160 nm in the lasing spectra of both broad-area and ridge waveguide lasers are reported. The bandgap-tuned lasers are assessed in terms of threshold current density, internal quantum efficiency, and internal losses. The ON/OFF ratios of bandgap-tuned electroabsorption modulators were tested over a range of wavelengths, with modulation depths of 20 dB obtained from material which has been bandgap-shifted by 120 nm, while samples shifted by 80 nm gave modulation depths as high as 27 dB. Single-mode waveguide losses are as low as 5 dB · cm^{-1} at 1550 nm. Selective-area disordering has been used in the fabrication of extended cavity lasers. The retention of good electrical and optical properties in intermixed material demonstrates that PAID is a promising technique for the integration of devices to produce photonic integrated circuits. A quantum-well intermixing technique using a pulsed laser is also demonstrated.**

Index Terms—**III–IV semiconductors, InGaAs–InGaAsP, laser processing, optoelectronic integration, photonic integrated circuits, quantum-well intermixing.**

I. Introduction

INCREASINGLY, the demand for higher data rate systems is pushing optical communication technology toward monolithic integration of source and modulator devices operating at wavelengths around 1.55 μm, at which wavelength the propagation loss in silica fibers is a minimum. For similar reasons, there is much interest in photonic switching circuits requiring low-loss waveguides coupled to modulators. Other considerations such as improved mechanical stability and reliability, as well as the general reduction in size, makes integration of devices a significant goal. The use of MQW electroabsorption modulators [1], employing the quantum-confined Stark effect (QCSE), for example, offers higher speed operation than does direct modulation of a laser source. During recent years, the InGaAs–InGaAsP–InP-based semiconductor multiple-quantum-well (MQW) system has found a major role in the fabrication of photonic devices.

In order for photonic integrated circuits (PIC's) to be realized, the ability to exercise control over local optical and electrical characteristics of the MQW material across a wafer is of fundamental importance. Many techniques are currently under investigation to this end. Those based on selective regrowth appear promising, but expensive facilities such as metal organic chemical vapor deposition (MOCVD) are needed during the entire production process [2]. Other approaches are based on quantum-well intermixing (QWI).

In a QW system, a permanent change in the absorption edge can be accomplished by intermixing the wells and barriers in order to alter the well width and potential barrier height, the values of which determine the energy of the quantum-confined states relative to the bulk bandgap. In the limit of complete intermixing, a semiconductor alloy, with the average composition of the wells and barriers, is formed but less extreme intermixing produces structures of intermediate bandgap in which the 2-D properties of the QW layers are partially retained. However, intermixing is only of use if it can be localized to particular areas of the wafer, and if the electrical and optical qualities of the processed material are adequate for use in devices.

Intermixing of MQW structures can also be used to shift the gain envelope of "as-grown" material to allow lasers, with a range of tuned wavelengths, to be fabricated from a single wafer with particular applications in wavelength-division multiplexing (WDM) and instrumentation.

The first intermixing studies were performed on GaAs–AlGaAs structures, and since then various methods have been developed. These methods have been applied

Manuscript received November 13, 1995; revised July 2, 1996. This work was supported by the Engineering and Physical Sciences Research Council (U.K.) under Grant GR/G13488. The work of A. McKee was supported by an EPSRC CASE studentship with DRA (Malvern). The work of G. Lullo was supported by the Italian MURST.

A. McKee, C. J. McLean, A. C. Bryce, R. M. De La Rue, and J. H. Marsh are with the Optoelectronics Research Group, Department of Electronics and Electrical Engineering, University of Glasgow, Glasgow G12 8QQ, Scotland, U.K.

G. Lullo is with the Optoelectronics Research Group, Department of Electronics and Electrical Engineering, University of Glasgow, Glasgow G12 8QQ, Scotland, U.K., on leave from the Dipartimento di Ingegneria Elettrica, Università di Palermo Viale delle Scienze, I-90128 Palermo, Italy.

C. C. Button is with the Department of Electronic and Electrical Engineering, University of Sheffield, Sheffield S1 3JD, U.K.

Publisher Item Identifier S 0018-9197(97)00350-3.

to the InGaAs–InGaAsP system with varying degrees of success. Impurity-induced disordering (IID) using diffusion of impurities from the surface [3], IID using ion implantation and annealing [4], [5], and impurity-free vacancy disordering (IFVD) [6] have all been investigated. The first two methods require the introduction of impurities into the device structure which can degrade the device performance, particularly if the impurities are electrically active. For all the above techniques, selective area intermixing can be achieved using standard lithographic techniques to pattern suitable masks. Also, all the methods use an annealing stage, either in a conventional furnace or in a rapid thermal processor, which limits their usefulness in the InGaAs–InGaAsP QW system. This material system has poor thermal stability: conventional furnace annealing of as-grown structures at temperatures as low as 550 °C can cause significant intermixing. Rapid thermal processing allows the use of higher temperatures (≈700 °C). The thermal stability varies from wafer to wafer; this variation is thought to be related to the etch pit density of the substrate on which the structure is grown [7]. This poor thermal stability results in limited shifts or bandgap shifts are incurred to differing degrees over all parts of the wafer [6].

In the GaAs–AlGaAs system, laser-induced disordering techniques have been investigated and shown to be effective [8], [9]. These laser-induced processes require high-power densities to melt the material, but the quality of the recrystallized material may be poor [10] and can introduce thermal shock damage if used in high-energy pulsed mode.

Photoabsorption-induced disordering (PAID) is a promising new QWI process for the InGaAsP system which uses laser annealing [11]. This process takes advantage of the poor thermal stability of the InGaAsP system and, essentially, involves band-to-band absorption of the incident laser photons within the active region of a multilayer structure. Subsequent carrier cooling and nonradiative recombination results in the generation of heat. Blue-shifts of the photoluminescence (PL) peak energy of greater than 100 meV, in standard MQW laser structures, are obtainable. The method is impurity-free, requires only a fraction of the power densities of existing CW techniques (~1–10 W · mm^2 compared with 10^5 W · mm^{-2}), and does not involve a melt phase in the semiconductor processing. An advantage of this technique is that it is layer composition selective, which is additionally advantageous in that it is not restricted to near-surface layers.

The bandgaps of InP, $In_{1-x}Ga_xAs_yP_{1-y}$ (lattice-matched with $x = 0.19$ and $y = 0.37$) and $In_xGa_{1-x}As$ ($x = 0.53$) are 1.35, 1.084, and 0.72 eV, respectively, [12] and hence InP is effectively transparent to the laser at 1.064 μm (1.165 eV), but radiation is absorbed in the other layers.

In the following sections, we will describe the fabrication and assessment of various PIC components, i.e., lasers, waveguides, and modulators, so demonstrating that PAID is a promising technique for the realization of functional optoelectronic circuits.

II. Experimental Procedure

During the disordering process, material is coated with a layer of plasma-deposited silicon dioxide which acts both as an antireflection coating and as a protective layer against surface reactions with the atmosphere. It also prevents the desorption of P from the sample. It has been found that a layer around 500 nm thick (corresponding to $3\lambda_{YAG}/4n_{SILICA}$) is sufficient to protect the surface during the high-temperature anneal. It has been found that annealing this material system with a SiO_2 cap at the temperatures used here does not cause impurity-free vacancy disordering [13].

The material is placed on polished ceramic on a hotplate at around 220 °C. This increase in the background temperature of the sample significantly reduces the incident laser power density required to heat the sample to a temperature at which disordering occurs. The use of the ceramic also reduces the required power density due to its poor thermal conductivity. The material is then irradiated with light from a CW Nd:YAG laser emitting at 1064 nm with a power density of around 5 W · mm^{-2} for times of around 30 min.

III. Bandgap-Tuned Oxide Stripe Lasers

Broad-area oxide stripe lasers were fabricated from standard MQW laser material which had been disordered by varying degrees in order to allow analysis of important properties such as threshold current density, internal quantum efficiency, and internal losses.

The laser structure investigated was grown by metal organic vapor phase epitaxy (MOVPE) on an (100)-oriented n^+-type InP substrate and consisted of five 85-Å InGaAs wells with 120-Å InGaAsP ($\lambda_g = 1.26$ μm, where λ_g is the wavelength corresponding to the bandgap) barriers. The active region was bound by a stepped graded index (GRIN) waveguide core consisting of InGaAsP confining layers. The thicknesses and compositions of these layers (from the QW's outward) were 500 Å of $\lambda_g = 1.18$ μm and 800 Å of $\lambda_g = 1.05$ μm. The structure, which was lattice-matched to InP throughout, was completed by a 1.4-μm-thick InP upper cladding layer and a 0.2-μm-thick InGaAs contact layer. The first 0.2 μm of the upper cladding layer was doped with Zn to a concentration of 5×10^{17} cm^{-3} and the remaining 1.2 μm to 2×10^{18} cm^{-3}. The lower cladding layer was Si doped to a concentration of 1×10^{18} cm^{-3}. The waveguide core was undoped, thus forming a pin structure with the intrinsic region restricted to the QW's and the GRIN layers.

The SiO_2 caps were removed after disordering, and windows 85 μm wide with a 300-μm pitch were opened in a new 200-nm-thick passivation layer of SiO_2 using routine photolithographic techniques. The samples were then thinned and metal contacts (p-Ti–Au, n-Au–Ge–Au–Ni–Au) were evaporated onto both surfaces and annealed in a rapid thermal processor (325 °C for 90 s). Finally, the samples were scribed and cleaved into individual lasers with lengths ranging from 200 to 1000 μm.

Because a laser with a Gaussian beam profile had been used, the samples were not uniformly heated over their entire area. This resulted in less disordering around the edges of the samples compared with a more uniform central region. For this reason, there was a range of lasing wavelengths obtained from each sample, typically a spread of about 10 nm, therefore,

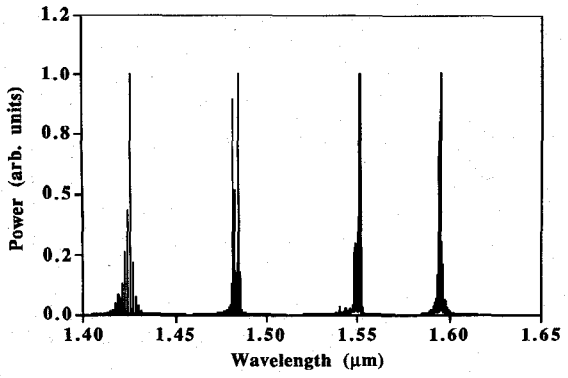

Fig. 1. Emission spectra of bandgap-tuned oxide stripe lasers.

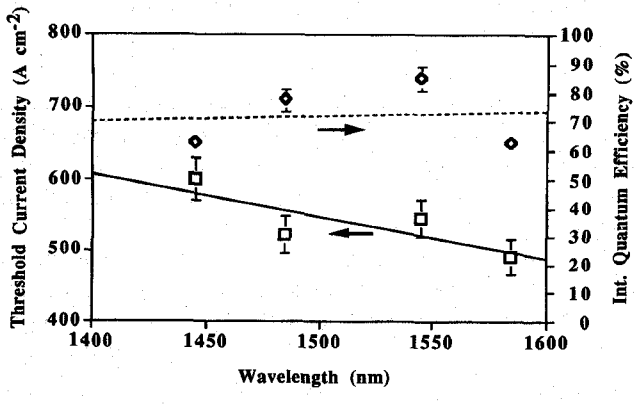

Fig. 2. Threshold current density and internal quantum efficiency of bandgap-tuned oxide stripe lasers.

only lasers from the centers of the samples were assessed. The uniformity of the intermixing would be improved by using a laser with a top-hat beam profile.

Fig. 1 shows output spectra from oxide stripe lasers fabricated from samples which have undergone different degrees of intermixing (blue shifted as much as 160 nm). These spectra were obtained from lasers operated in pulsed mode (400-ns pulse at a 1-kHz repetition rate) at 50% above threshold. It is apparent that the gain envelope of the material has not been measurably broadened, indicating that all wells are disordering equally, irrespective of their depth within the epitaxial structure. This is to be expected because of the thermal nature of the disordering process and the close spacing of the wells.

Lasers with the lowest threshold currents and best external quantum efficiencies were chosen to determine the device and material parameters. The inverse of the slope efficiency was plotted against cavity length for each sample. From the slope of such plots, the internal loss can be inferred and the intercept on the y axis gives the reciprocal of the internal quantum efficiency. It is difficult to obtain precise values of the internal efficiency by this technique without a very large data set (here, five lasers were measured for each of five cavity lengths at each wavelength), especially when using pulsed measurements, but trends can readily be inferred. Fig. 2 shows the threshold currents and internal quantum efficiencies of a range of disordered lasers.

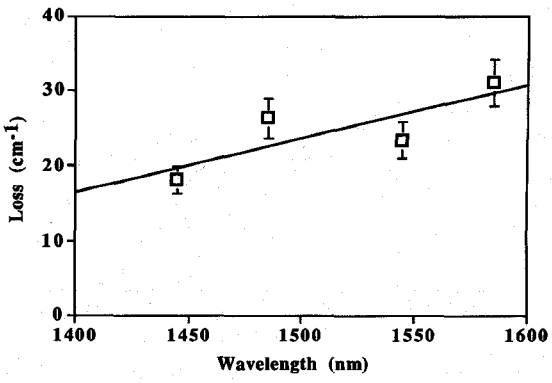

Fig. 3. Internal losses of bandgap-tuned oxide stripe lasers.

Several factors contribute to changes in the threshold current and quantum efficiency, e.g., alteration of the well shape, intermixing and dopant diffusion in the GRIN structure, and changes in the number of point defects within the material. The observed increases in the confinement factor and decrease in the internal losses will have the effect of reducing the threshold current density. The observed increase in threshold current is mainly due to the well shape changing and the electrons and holes becoming less confined within the wells, leading to the emission properties becoming closer to those of bulk material.

As discussed above, the absolute accuracy of the internal quantum efficiency data is likely to be limited. An initial increase in efficiency with intermixing is observed, followed by a drop. It is not clear how reliable these trends really are. It can, however, be inferred with certainty that the internal quantum efficiency remains substantially unaffected by the PAID process, i.e., the process does not appear to induce a significant number of nonradiative recombination centers.

Fig. 3 shows how the internal losses of the laser decrease as the material is disordered. The decrease is mainly due to a reduction in Auger effects and intervalence band absorption, as the lasing wavelength becomes shorter [14]. In addition, the free-carrier absorption coefficient is, to a first approximation, proportional to the square of wavelength (λ^2) [15] and so it will be reduced by around 20% over the range of wavelength studied. Another factor to note is that the guided mode will become more strongly confined within the active region of the laser as the wavelength is reduced [16].

The results demonstrate that no apparent losses are incurred because of dopant diffusion (Zn) into the active region, a conclusion which is also supported by the observation that the internal loss decreases with increasing intermixing. This is an important point, as a displaced p–n junction due to diffusion of dopants would seriously reduce the performance of devices fabricated by intermixing.

IV. Electroabsorption Modulators

The material used to fabricate the electroabsorption modulators was identical to that used to fabricate the bandgap-tuned lasers with the excitonic peak of the as-grown material, measured by photoluminescence at room temperature, occurring at approximately 1580 nm.

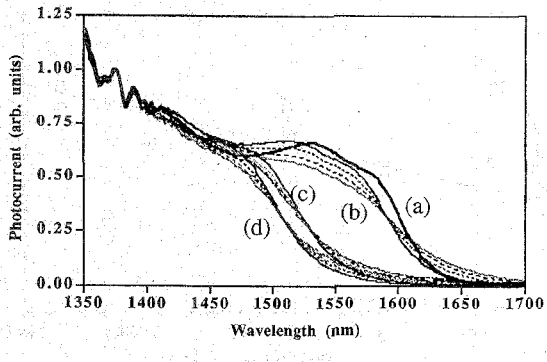

Fig. 4. Photoconductivity spectra for samples under 0 V (——), 0.5 V (– – –), 1 V (- - - - -), and 1.5 V (· · · · · ·) reverse bias, which have undergone intermixing of: (a) 0 nm (control), (b) 10 nm, (c) 63 nm, and (d) 78 nm.

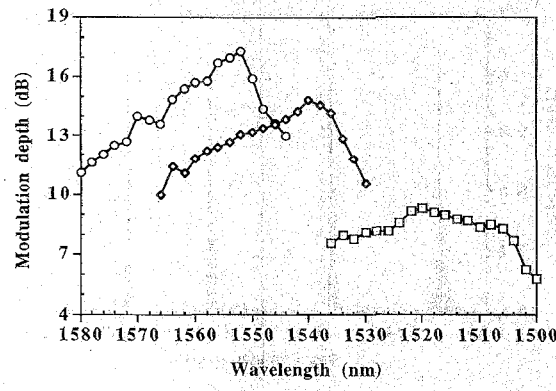

Fig. 5. Modulation depth when bias voltage was varied between +0.5 V and −1 V plotted as a function of wavelength for three samples which had undergone different bandgap shifts: —○— shifted 80 nm, —◇ shifted 95 nm, and —□— shifted 120 nm.

Photocurrent (PC) measurements were carried out to determine the suitability of the material for use in modulators. Fig. 4 shows PC measurements of disordered and undisordered material under various reverse bias conditions. In the case of the control sample, although no clear excitons were observed, features corresponding to the light and heavy hole transitions are distinguishable. For the intermixed samples, these features become more poorly defined as the extent of disordering increases, and quickly merge to form a single absorption edge. Another clearly defined feature in Fig. 4, at ~1.37 μm, corresponds to optical absorption by atmospheric water molecules. Due to run-to-run variations, all photocurrent spectra have been normalized at the water absorption feature. In each case, the PC spectrum clearly indicates increased absorption at longer wavelengths resulting from a broadening of the absorption edge on application of a reverse bias. As a consequence of the excitons being poorly resolved even in the control sample at zero bias, it is not clear whether or not there is any appreciable demonstration of the quantum-confined Stark effect, however, the broadening of the absorption edge shows there is a substantial Franz–Keldysh (FK) effect. Even with the limited absorption changes observed, useful waveguide modulators could be fabricated.

Four-μm-wide, strip-loaded, single-mode waveguides were fabricated parallel to the [011] direction. About 0.8 μm of the InP upper cladding layer was etched by CH_4-H_2 reactive ion etching, in order to prevent any possible damage to the MQW structure. The etching was completed using a $HCl:H_3PO_4$ wet etch which, as a consequence of crystal orientation [17], gave vertical and smooth waveguide sidewalls. Following the deposition of a 200-nm-thick SiO_2 passivation layer, contact windows were opened around the ridges. The samples were then thinned and metal contacts, using the same metals as were used for the lasers, were evaporated which were annealed at 400 °C for 60 s using a rapid thermal processor. The samples were then cleaved to a length of 500 μm.

A semiconductor laser, tunable in the wavelength range from 1480 to 1580 nm, was used to assess the device performance. Light was end-fire coupled into the sample through a tapered microlensed single-mode fiber. A fiber polarization rotator ensured that only the TE-mode was excited in the waveguides. The output from the sample was collected by another fiber and detected by a germanium photodiode. Transmission characteristics were investigated as a function of wavelength. Assuming a coupling loss of 6 dB at the sample facets, the estimated propagation loss of the modulators at the optimum operating wavelength with no applied bias was about 2 dB per 100 μm.

Fig. 5 shows the modulation depth versus wavelength for three different degrees of disordering, corresponding to a shift in the absorption edge, with respect to the as-grown material, of 80, 95, and 120 nm. Measurements were carried out with a voltage sweep between +0.5 V and −1 V. A decrease in the modulation depth is clearly noticeable in samples which have increased disordering. Such behavior is in good agreement with theoretical expectation, as disordering causes a reduction in quantum confinement due to the smoothing of the potential barrier shape. This effect is worthy of further investigation because the use of shallow wells has been suggested as a solution for increasing the saturation intensity in electroabsorption modulators [18]. Moreover, because shallow wells prevent hole pile-up in the active region, a higher cut-off frequency at low bias voltages and an improvement in quantum efficiency should be allowed. The reduction in the modulation depth could also be attributed to defects generated in the intermixing process, however, the high quality of the bandgap-tuned lasers indicates that the number of such defects is not significant.

At the optimum modulation wavelength of 1522 nm for samples whose bandgap had been shifted as far as 120 nm, an ON/OFF ratio of over 20 dB (Fig. 6) was obtained when the bias voltage was varied between +0.5 V and −2.5 V. This is further evidence that the PAID process does not produce any dramatic degradation in the optical and electrical properties of the MQW structure. Samples disordered to a lesser degree (80 nm) gave higher ON/OFF ratios of at least 27 dB at 1555 nm, limited by the low intensity of light available at longer wavelengths.

A forward bias of about +0.5 V was found to increase the output power from the modulators, typically by 5 dB. Because this voltage is well below the diode turn-on voltage, only a very small current actually flows through the device. This implies that no amplifying effect can account for such an increase in the output power. Most likely, the small forward

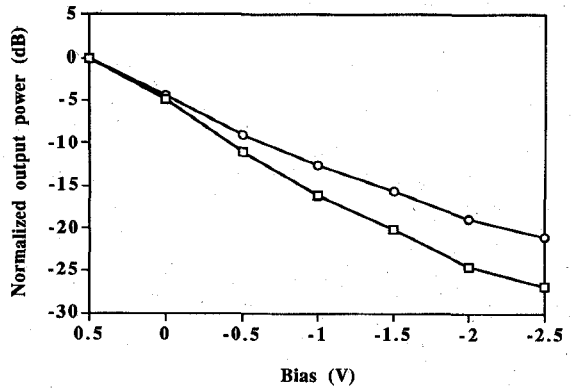

Fig. 6. Normalized output power as a function of bias for two samples which had undergone different bandgap shifts: (a) shifted by 120 nm and measured at 1522 nm, and (b) shifted by 80 nm and measured at 1555 nm.— ○ — sample (a), —□— sample (b).

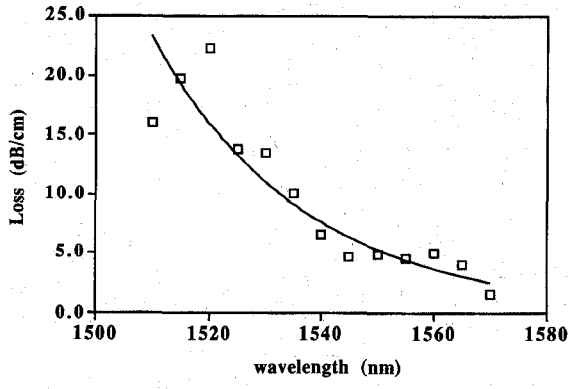

Fig. 7. Single-mode ridge waveguide losses.

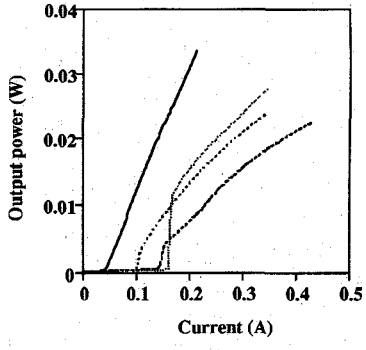

Fig. 8. Characteristics of simple and extended cavity lasers with a 400-μm active section and 0- (_____), 400- (·····), 800- (- - - - -), and 1200- (~~~~) μm passive section.

bias neutralizes the built-in potential between the doped layers which form the p-i-n structure.

V. Low-Loss Waveguides

The material used to measure waveguide losses was similar to that of the standard MQW laser material described above, except that there were no dopants introduced during growth and the upper cladding was 1.5 μm of InP and the InGaAs contact layer was omitted. The material was disordered from a starting room-temperature PL wavelength of 1585 to 1380 nm, corresponding to total intermixing between the wells and the barriers.

Single-mode strip-loaded ridge waveguides of width 2 μm were then fabricated parallel to the [011] direction on the disordered material as described previously. The waveguide losses were measured over a range of wavelengths from 1510 to 1570 nm using the Fabry–Perot technique [19]. The light source used was a tunable single-mode semiconductor laser.

Fig. 7 shows the single-mode waveguide loss as a function of wavelength. Losses in this material should be quite low as the band-edge of the material has been shifted by a substantial amount. At higher wavelengths (lower energy), the losses will be mainly due to scattering, leakage from the guide, and absorption losses from imperfections in the material. At shorter wavelengths, the losses will rise as the tail of the band edge is encountered and absorption increases. It is evident from this graph that the losses are very low with a value of 5 dB · cm^{-1} at a wavelength of 1550 nm, the wavelength at which integrated devices in the InP system will operate. A possible reason for the low loss is that no impurities are introduced at any stage during the PAID process which could increase the absorption loss or cause damage in the crystal structure and increase the scattering losses. The upper cladding layer in this structure is undoped, but in an active device the layer would be doped p-type with a concentration of about 5×10^{17} cm^{-3}. It is estimated [20] that the effect of this doping concentration in an InP cladding layer would be to increase the losses to about 15 dB · cm^{-1}. These results demonstrate that PAID is an effective way of producing low-loss interconnecting waveguides for use in photonic integrated circuits.

VI. Extended Cavity Lasers

Having demonstrated the effectiveness of PAID in the fabrication of various individual PIC components, a simple integrated device was fabricated, incorporating both an active and a passive section.

The material used in the fabrication of these devices was of a similar layer structure to those already mentioned, except that the wells were slightly narrower, resulting in a shorter emission wavelength of 1500 nm. As it was decided that ridge type lasers should be fabricated, it was also desirable to assess the lasing characteristics of standard, i.e., all active area, ridge devices fabricated from as-grown material. The 4-μm-wide ridges were etched by wet chemical etching to a depth of 1.5 μm where the etch stopped at the confinement layers. Lasers with cavity lengths of 400 and 800 μm were assessed and found to have threshold currents of 20 and 30 mA, respectively, and linear light-current (P–I) characteristics.

Before disordering, the InGaAs contact layer was removed from the passive sections of the extended cavity laser (ECL) samples, and SiO_2 was deposited as usual. The laser was focused to a 2.5-mm diameter spot, with a power of 8 W, and scanned across the passive section. Ridge lasers were then fabricated in the same fashion as before, with 400-μm-long active, and 0-, 400-, 800-, and 1200-μm-long passive sections. The P–I characteristics of these lasers are shown in Fig. 8.

The curve for the zero passive length laser has typical characteristics, although the threshold current is somewhat higher than that previously obtained, this higher current being due

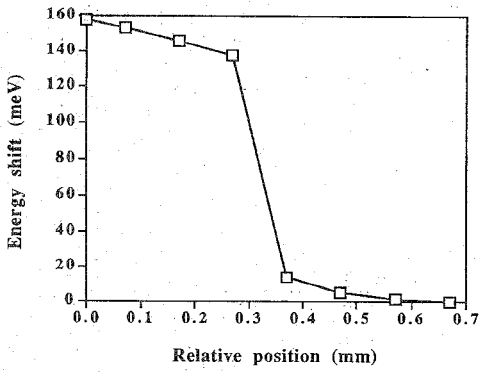

Fig. 9. Room-temperature photoluminescence peak energy shift as a function of position across the interface of a gold reflection mask.

to larger ridge widths. For the ECL's, however, the threshold currents were much higher, over 100 mA, and the P–I curves include what appears to be a vertical jump in output, prior to the expected linear dependence. Such a P–I curve is typical of a Q-switched laser, with a saturable absorber in the cavity which must be bleached before lasing can take place. This implies that there is a highly absorbing unpumped region at the interface which has not been sufficiently intermixed to prevent substantial absorption. The spatial selectivity of the disordering process has been determined using a gold reflection mask. Here, the degree of intermixing ranged from 157 meV for the unmasked area to zero over a distance of 600 μm, although the majority of this variation (10%–90% points) occurred across a narrower 100-μm region (Fig. 9). This poor spatial resolution is certainly sufficient to be responsible for the characteristics observed above.

By extrapolating the P–I curves back to the x axis, it is possible to define an effective threshold current for the devices. These currents can be fitted to the expression [21]

$$\ln\left(\frac{I_{th}}{I_{0th}}\right) = \frac{1}{G_0 \cdot L_a}(\alpha_p \cdot L_p - \ln k) \tag{1}$$

from which the passive section loss can be obtained. $I_{\rm th}$ and I_{0th} are the threshold currents for lasers with and without passive sections, G_0 is the gain factor (calculated from zero length passive section lasers), L_a and L_p are the lengths of the active and passive sections, respectively, α_p is the loss in the passive section, and k is the coupling coefficient between the sections (assumed to be unity in this case). The calculated passive section loss is 28.7 cm^{-1}, this value representing the average loss through the passive section, including the very highly absorbing region next to the active section.

VII. Thermal Modeling of Laser Heating

In the previous sections, it has been shown that PAID is an extremely successful intermixing method when applied to the production of individual devices. In order to determine the limits of the technique as a means of fabricating complex integrated systems, it is necessary to know the extent of the lateral conduction of heat in the semiconductor material. For this reason, detailed thermal modeling has been undertaken. Additionally, the thermal dependence of the disordering rate

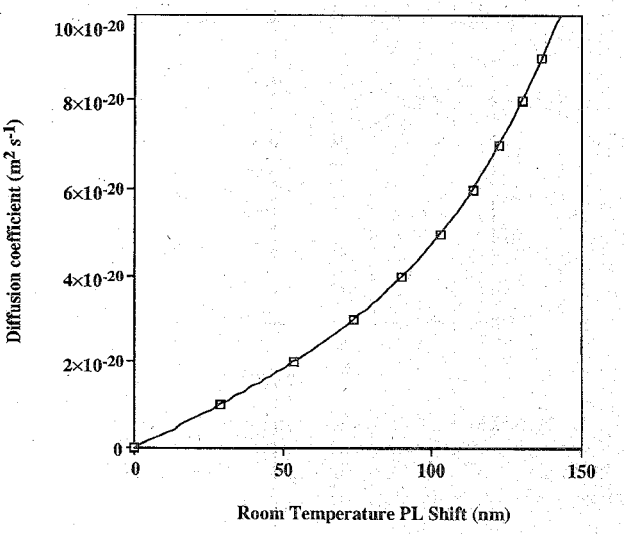

Fig. 10. Diffusion coefficients as a function of PL shift, determined from solution of Schrödinger's equation across a diffused well.

must be quantified in order to relate the thermal distribution to an intermixing profile. To do this accurately, material was annealed in a rapid thermal processor (RTP) over a range of temperatures, and the resultant photoluminescence (PL) peak shift was measured. Since the temperature and anneal times are predetermined and the material parameters are known, diffusion coefficients can be calculated.

The software used for the thermal conduction simulations was a commercially available finite element package called ABAQUS, written in FORTRAN, designed to solve complex nonlinear mechanical problems. The program has the capacity for simulation of both steady-state and transient heat flow.

For the simulation of laser heating of semiconductor material, several simplifications and assumptions have been made. Initially, the models were restricted to the 2-D case which is adequate for the investigation of simple interface problems and significantly reduces processing time. Also, although typical device material has epitaxially grown layers of InGaAs and InGaAsP ($\approx$0.35 μm), which possess different heat conduction properties to InP [22], it is assumed these layers are sufficiently thin that they can be ignored and, therefore, that the material investigated is purely InP. Further, it is assumed that the base of the sample is at a fixed temperature, i.e., there is perfect thermal contact between the sample and an infinite heat sink, which in practice was not the case.

The temperature dependence of the thermal conductivity [23] (K) of the doped InP substrates was taken into account using the relationship

$$K = 2168 \times T^{-1.45}\mathrm{W} \cdot \mathrm{cm}^{-1} \cdot \mathrm{K}^{-1} \tag{2}$$

where T is in Kelvin in all the simulations.

In order to model the intermixing, it was assumed that wells and barriers intermix according to a standard diffusion model, and hence the disordered quantum-well profile can be represented by a superposition of error functions [24]. Schrödinger's equation can then be solved across the well, to determine the energy levels. Using a computer model, the diffusion coefficient was determined as a function of

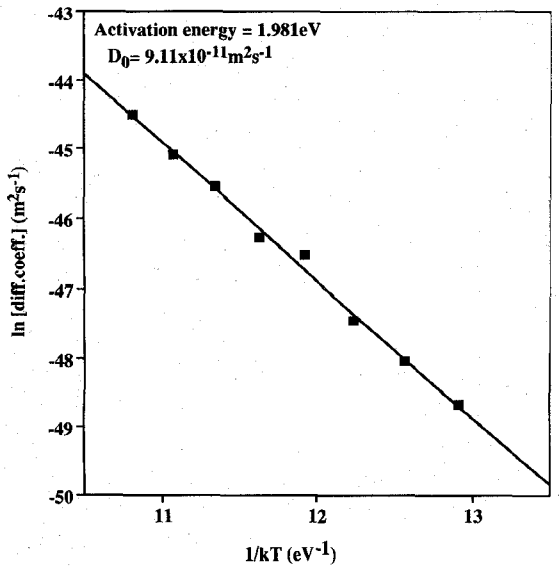

Fig. 11. Arrhenius plot of diffusion coefficients calculated from anneal test data.

wavelength shift for MQW waveguide material. A fixed time of 90 s was adopted. Fig. 10 shows the diffusion coefficient, D, plotted as a function of PL shift, $\Delta\lambda$.

A fourth-order polynomial curve was fitted to this data which gave a relationship between D and $\Delta\lambda$ as

$$D = 2.04 \times 10^{-28}(\Delta\lambda)^4 - 2.43 \times 10^{-26}(\Delta\lambda)^3 + 2.15 \times 10^{-24}(\Delta\lambda)^2 + 2.97 \times 10^{-22}(\Delta\lambda) + 2.60 \times 10^{-23}. \quad (3)$$

An RTP anneal test of the material was then performed over a temperature range of 600 to 800 °C for 90 s. The initial and final energies were determined from PL measurements. Using (3), the diffusion coefficient was calculated for each temperature used in the anneal test (Table I). Since D and T are related by

$$D = D_0 \exp\left(-\frac{E_A}{kT}\right) \quad (4)$$

D_0 and E_A can be found from the Arrhenius plot of $\ln(D)$ as a function of $1/kT$ (Fig. 11). The intercept of the line with the y axis gives D_0, which is equal to 9.11 $\times$ 10^{-11} m^2 s $^{-1}$ while the gradient of the graph gives the activation energy, E_A, as 1.981 eV.

Once all the constants are known, it is possible to calculate the PL shift of the material for any time and temperature using the same program.

The data presented above can now be combined with a steady-state temperature profile to determine the resolution of the process or the "transition region" between disordered and undisordered material. It is assumed that the laser has a Gaussian beam profile with its center incident on the interface between exposed and masked areas and, therefore, only half the total power is absorbed. It is further assumed that all

TABLE I
DIFFUSION COEFFICIENT AS A FUNCTION OF ANNEAL TEMPERATURE

Anneal Temperature (°C)	Shift in PL wavelength (nm)	Diffusion Coefficient (m^{2}s^{-1})
600	0	2.60 x 10^{-23}
625	2.3	7.21 x 10^{-22}
650	4.4	1.37 x 10^{-21}
675	7.8	2.46 x 10^{-21}
700	18.8	6.24 x 10^{-21}
725	23.8	8.06 x 10^{-21}
750	45.8	1.67 x 10^{-20}
775	66.6	2.62 x 10^{-20}
800	99.6	4.70 x 10^{-20}

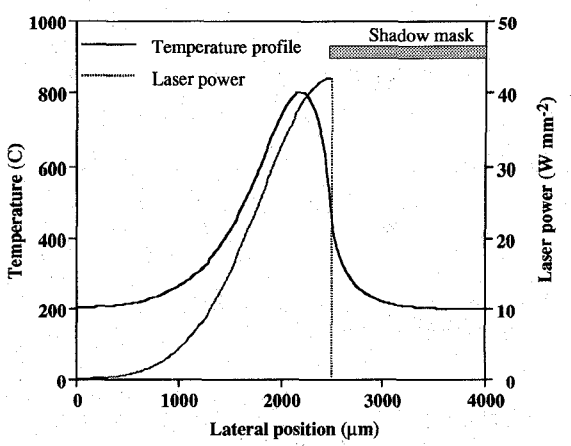

Fig. 12. Incident laser beam profile and corresponding temperature profile.

absorption occurs in the topmost layer of the material. For this model, the boundary condition for the base of the sample is T = 200 °C. The input power has been chosen such that the maximum temperature reached is 800 °C which requires an average intensity of 24 W · mm^{-2} for a laser beam with a full width at half maximum (FWHM) of 1.66-mm diameter (corresponding to a width at $1/e$ of 2 mm). The peak value of 800 °C was chosen as it is known to cause a PL shift of approximately 100 nm for a 90-s anneal in the RTP. This shift is typical of that obtained when the sample has been irradiated by the laser for ≈3 min in the PAID process.

Fig. 12 shows the input beam profile and the calculated temperature profile induced by it. It is evident that the peak temperature is displaced from the position of the peak laser intensity as heat generated close to the mask diffuses underneath it. The temperature gradient under the mask is greater than that on the irradiated side, reflecting the abrupt nature of the incident power gradient.

The simulation was repeated for different heat sinking conditions. With a heat-sink temperature of 350 °C, the incident intensity required to produce a maximum temperature of 800 °C was 15 W · mm^{-2} while only 8.5 W · mm^{-2} was required when the base of the sample was fixed at a temperature of 500 °C. Fig. 13 shows the PL shift across the masked interface, determined from the temperature profile for the three different heat-sinking conditions. The threshold

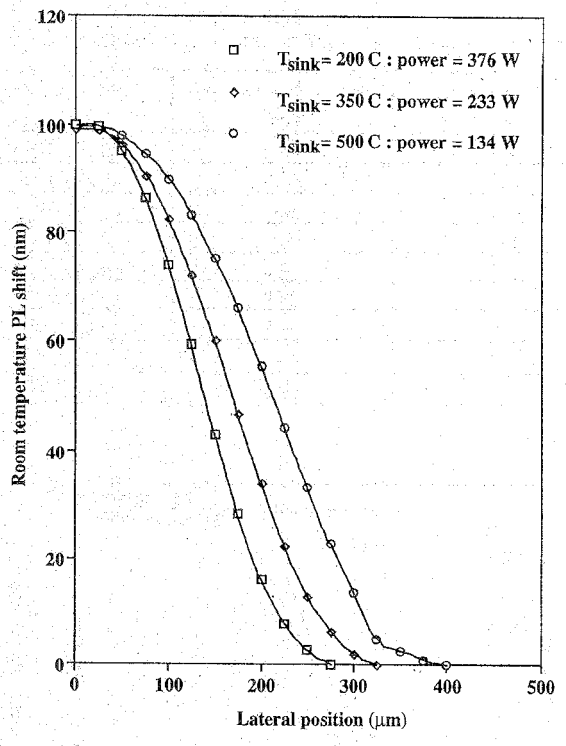

Fig. 13. Disorder profile, as calculated from the simulated temperature distribution and diffusion coefficients.

value and the nonlinear nature of the shift as a function of temperature result in a rather narrow disordered region. Further studies determined the effect of varying the beam size. The size of the transition regions for three heat-sinking conditions and three spot sizes are shown in Fig. 14. The resolution was considered to be the lateral distance between 10–90% of maximum disordering. If we also consider that the peak shift in the profile is displaced from the mask interface, it is clear that, in the case of ECL's, there can be a significant length of undisordered, or partially disordered, absorbing material within the cavity.

VIII. Pulsed Laser Disordering

Although PAID has been demonstrated to be an effective disordering technique, the spatial selectivity of the technique is limited by thermal conduction which leads to a lateral heat flow, as illustrated above. An alternative laser technique, utilizing high-energy pulses, has recently been reported [25].

Absorption of an incident energy pulse leads to localized transient heating in the semiconductor crystal and rapid thermal expansion. The resultant disruption to the lattice leads to an increase in the density of defects. These point defects subsequently diffuse during a high-temperature anneal, so enhancing the QW intermixing rate.

Computer simulations of the temporal evolution of thermal transients, using ABAQUS, have revealed that InP has a thermal time constant of the order of nanoseconds, therefore, in order to restrict the dissipation of heat and generate highly localized temperature spikes, heating on a similar short time scale is required. A Q-switched Nd:YAG laser,

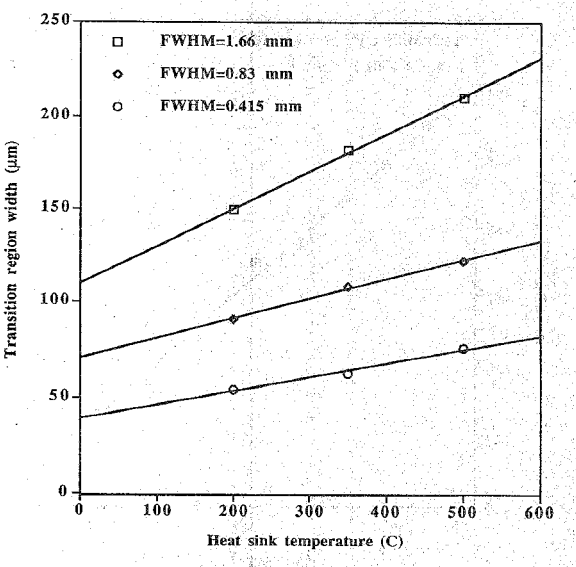

Fig. 14. Calculated transition widths, between disordered and undisordered areas, as a function of the laser beam width, and the temperature of the heat sink.

generating pulses ~20 ns was employed. As with PAID, the InP substrate and cladding material are transparent at the laser wavelength.

The sample material was an undoped structure, grown by MOVPE, similar in layer composition to those described earlier. Spatially selective PL measurements were performed at 77 K using a fiber probe, with a core diameter of 50 μm, placed in contact with the sample surface. The samples were immersed in a bath of liquid nitrogen which was mounted on a translation stage. Luminescence was collected by the same probe fiber and monitored via a Y-coupler. The PL pump source was a CW Nd:YAG laser operating at 1.064 μm.

Samples were irradiated with the Q-switched laser at room temperature and at normal incidence to the surface, with 600–9000 pulses. The pulse repetition rate was 10 Hz and the energy density ~5 mJ $\cdot$ mm^{-2}. The energy density was chosen to be just below the threshold at which surface damage occurred. The samples were then annealed repeatedly in an RTP at 700 °C, in conjunction with an unirradiated control sample. Earlier anneal tests had indicated that the material was essentially thermally stable for short anneal times at this temperature. A 200-nm layer of SiO_2 was deposited on all samples prior to annealing in order to prevent desorption from the surfaces. PL measurements were carried out after each anneal. The resultant peak wavelengths are plotted as a function of the total anneal time and the number of irradiating pulses (Fig. 15).

It is apparent that the differential shift in the peak PL wavelength between those samples exposed to the pulsed laser and the control sample is significant. The wavelength shift in the control sample after a total annealing time of 240 s at 700 °C is only 10 nm in comparison with the exposed samples which ranged in total shift between 123 and 180 nm.

It can be seen that, after a large initial effect, the overall shift is not a strong function of the number of incident pulses. This is believed to be due to the agglomeration of point defects,

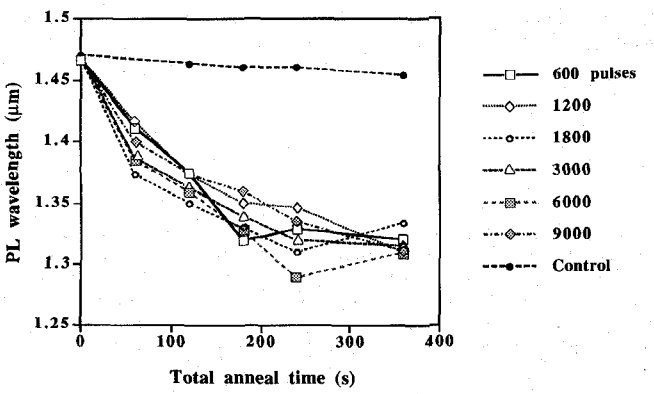

Fig. 15. Peak PL wavelength after annealing for various times at 700 °C. The effect of different numbers of laser pulses is also plotted.

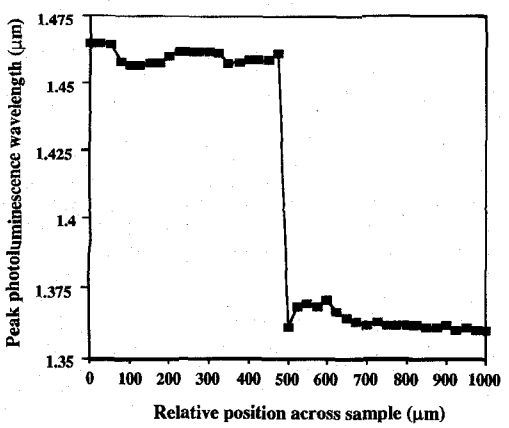

Fig. 16. Spatially resolved PL across an annealed sample of which only half was exposed to the laser pulses. The resolution is limited by that of the PL system (~25 μm).

generated during the exposure to the laser pulses, into extended defects which inhibit diffusion [26].

To measure the spatial resolution of the intermixing, material was irradiated for 20 min under the above conditions, but in this case, a portion of the sample was shielded from the laser with a metal mask, suspended a few hundred microns above the surface. After annealing, again at 700 °C for 180 s, the 77-K PL peak wavelengths were measured along a line perpendicular to the masked interface. Fig. 16 shows the variation in the peak wavelength recorded as a function of position across the interface in steps of 25 μm. Measurement of the ultimate resolution is limited by the probe size of the present PL arrangement. The undulations in the plot may be evidence of diffraction of the laser light at the mask interface. This effect will be reduced by using gold reflective masks evaporated directly onto a silica-coated surface.

IX. Conclusion

Photoabsorption-induced disordering has been demonstrated to be an effective quantum-well intermixing technique for producing controllable bandgap tuning in the InGaAs–InGaAsP system. This bandgap tuning has been utilized in the fabrication of different devices from standard MQW laser material. The process displays significant advantages over existing techniques. It is not restricted to disordering of structures with surface or near-surface multilayers, as it is not limited by the extent of diffusion of surface impurities into the material or by ion-implantation ranges, although the upper cladding layers of the structure should preferably be transparent at the laser wavelength.

Single-mode waveguide losses as low as 5 dB · cm^{-1} have been measured at 1.55 μm. Lasers have been fabricated from material intermixed using the process with blue shifts in the lasing spectra of 160 nm. The threshold current densities and internal quantum efficiencies, being comparable to that of the as-grown material, indicate that the material is still of excellent quality for use in the integration of devices.

Photoconductivity spectra demonstrate that the electrical and optical qualities of partially intermixed material is sufficiently high that it can be used to form electroabsorption modulators based on the QCSE and FK effects. Bandgap-tuned electroabsorption ridge waveguide modulators have been fabricated in an InGaAs–InGaAsP MQW structure which had been disordered. ON/OFF ratios of up to 27 dB have been measured in 500-μm-long devices.

The first steps toward integration have been taken with the fabrication of extended cavity lasers, although problems still exist at the interfaces. This may be combated by overlapping the active section contact with the passive section to ensure all undisordered material is pumped.

We have also demonstrated that pulsed laser irradiation at 1.064 μm can substantially alter the local thermal stability of the InGaAs–InGaAsP material system. Subsequent annealing has allowed bandgap increases of ~100 meV to be realized. The spatial resolution of the process was measured to be better than 25 μm, a value which is limited by the resolution of the PL system. The spatial resolution of the pulsed laser process is at least adequate for the realization of photonic integrated circuits.

Acknowledgment

The authors wish to thank K. C. Byron and C. J. Armistead at BNR Europe, Ltd., for providing access to a tunable semiconductor laser, and J. S. Roberts and C. C. Button of the University of Sheffield for providing epitaxial layers. Thanks also to K. W. D. Ledingham of the Department of Physics and Astronomy for providing access to the Q-switched laser, and M. W. Street for the use of his Schrödinger solver program.

References

[1] T. H. Wood, "Multiple quantum well (MQW) wave-guide modulators," *J. Lightwave Technol.*, vol. 6, pp. 743–757, 1988.

[2] M. Aoki, M. Suzuki, H. Sano, T. Kawano, T. Ido, T. Taniwatari, K. Uomi, and A. Takai, "InGaAs/InGaAsP MQW electroabsorption modulator integrated with a DFB laser fabricated by band-gap energy control selective-area MOCVD," *IEEE J. Quantum Electron.*, vol. 29, pp. 2088–2096, 1993.

[3] S. A. Schwarz, P. Mei, T. Venkatesan, R. Bhat, D. M. Hwang, C. L. Schartz, M. Koza, L. Nazar, and B. J. Skromme, "InGaAs/InP superlattice mixing induced by Zn or Si diffusion," *Appl. Phys. Lett.*, vol. 53, pp. 1051–1053, 1988.

[4] B. Tell, J. Shah, P. M. Thomas, J. W. Sulhoff, K. F. Brown-Goebler, A. D. Giovanni, B. I. Miller, and U. Koren, "Phosporus ion implantation induced intermixing of InGaAs/InP quantum well structures," *Appl. Phys. Lett.*, vol. 54, pp. 1570–1572, 1989.

[5] J. H. Marsh, S. A. Bradshaw, A. C. Bryce, R. Gwilliam, and R. W. Glew, "Impurity induced disordering in GaInAs quantum wells with barriers of AlGaInAs or of GaInAsP," *J. Electron. Mater.*, vol. 20, pp. 973–978, 1991.
[6] T. Miyazawa, H. Iwamura, and M. Naganuma, "Integrated external-cavity InGaAs/InP lasers using dielectric cap disordering," *IEEE Photon. Technol. Lett.*, vol. 3, p. 421, 1991.
[7] R. W. Glew, A. T. R. Briggs, P. D. Greene, and E. M. Allen, "The influence of the substrate on the thermal stability of InGaAs/InGaAsP quantum wells," in *Proc. 4th Int. Conf. InP and Related Materials*, Newport, RI, 1992, pp. 234–236.
[8] A. Rys, Y. Shieh, A. Compaan, H. Yao, and A. Bhat, "Pulsed laser annealing of GaAs implanted with Se and Si," *Opt. Eng.*, vol. 29, pp. 329–338, 1990.
[9] J. Ralston, A. L. Moretti, R. K. Jain, and F. A. Chambers, "Intermixing of $Al_xGa_{1-x}As$/GaAs superlattices by pulsed laser irradiation," *Appl. Phys. Lett.*, vol. 50, pp. 1817–1819, 1987.
[10] J. E. Epler, F. A. Ponce, F. K. J. Endicott, and T. L. Paoli, "Layer disordering of GaAs/AlGaAs superlattices by diffusion of laser incorporated Si," *J. Appl. Phys.*, vol. 64, pp. 3439–3444, 1988.
[11] C. J. McLean, J. H. Marsh, R. M. De La Rue, A. C. Bryce, B. Garrett, and R. W. Glew, "Layer selective disordering by photo-absorption induced thermal diffusion in InGaAs/InP based multiple quantum well structures," *Electron. Lett.*, vol. 28, p. 1117, 1992.
[12] S. Adachi, "Material parameters of $In_{1-x}Ga_xAs_yP_{1-y}$ and related binaries," *J. Appl. Phys.*, vol. 53, pp. 8775–8792, 1982.
[13] S. A. Bradshaw, J. H. Marsh, and R. W. Glew, "Very low loss waveguides formed by fluorine induced disordering of GaInAs/GaInAsP quantum wells," in *Proc. 4th Int. Conf. InP and Related Materials*, Newport, RI, 1992, pp. 604–607.
[14] N. K. Dutta, "Calculation of auger rates in a quantum well structure and its application to InGaAsP quantum well lasers," *J. Appl. Phys.*, vol. 54, p. 1236, 1983.
[15] R. G. Hunsperger, *Integrated Optics: Theory and Technology.* Berlin: Springer-Verlag, Springer Series in Optical Sciences, vol. 33, Springer-Verlag Electromagnetic.
[16] D. L. Lee, *Principles of Integrated Optics.* New York: Wiley, 1986.
[17] L. A. Coldren, K. Furuya, and B. I. Miller, "On the formation of planar-etched facets in GaInAsP InP double heterostructures," *J. Electrochem. Soc.*, vol. 130, pp. 1918–1926, 1983.
[18] F. Devaux, E. Bigan, A. Ougazzaden, B. Pierre, F. Huet, M. Carre, and A. Carenco, "InGaAsP/InGaAsP multiple-quantum-well modulator with improved saturation intensity and bandwidth over 20-GHz," *IEEE Photon. Technol. Lett.*, vol. 4, pp. 720–722, 1992.
[19] R. G. Walker, "Simple and accurate loss measurement technique for semiconductor optical wave-guides," *Electron. Lett.*, vol. 21, pp. 581–583, 1985.
[20] H. C. Casey and P. L. Carter, "Variation of the intervalance band absorption with hole concentration in p-type InP," *Appl. Phys. Lett.*, vol. 44, pp. 82–83, 1984.
[21] J. Werner, E. Kapon, N. G. Stoffel, E. Colas, S. A. Schwarz, C. L. Schwartz, and N. Andreadakis, "Integrated external cavity GaAs/AlGaAs lasers using selective quantum well disordering," *Appl. Phys. Lett.*, vol. 55, pp. 540–542, 1989.
[22] S. Adachi, "Lattice thermal resistivity of III–V compound alloys," *J. Appl. Phys.*, vol. 54, pp. 1844–1848, 1983.
[23] *Properties of Indium Phosphide,* INSPEC EMIS Datareviews Series no. 6.
[24] H. Peyre, F. Alsina, J. Camassel, J. Pascual, and R. W. Glew, "Thermal-stability of InGaAs/InGaAsP quantum wells," *J. Appl. Phys.*, vol. 73, pp. 3760–3768, 1993.
[25] C. J. McLean, A. McKee, G. Lullo, A. C. Bryce, R. M. De La Rue, and J. H. Marsh, "Quantum well intermixing with high spatial selectivity using a pulsed laser technique," *Electron. Lett.*, vol. 31, pp. 1285–1286, 1995.
[26] K. B. Kahen and G. Rajeswaran, "Study of the interdiffusion of GaAs-AlGaAs interfaces during rapid thermal annealing of ion implanted structures," *J. Appl. Phys.*, vol. 66, pp. 545–551, 1989.

Andrew McKee was born in Stranraer, Scotland, on May 3, 1970. He received the B. Eng. and Ph.D. degrees in electronics and electrical engineering from the University of Glasgow, Glasgow, Scotland, in 1992 and 1996, respectively.

He is currently working with Hewlett Packard Fiber Optics Components Operation in Ipswich, England, on high-performance quantum-well lasers.

C. J. McLean, photograph and biography not available at the time of publication.

Giuseppe Lullo received the diploma *cum laude* and the Ph.D. degree, both in electronic engineering, from the University of Palermo, Palermo, Italy, in 1990 and 1995, respectively. The subject of his thesis was the design and fabrication of a Mach–Zehnder electrooptic integrated modulator on LiNbO3. His Ph.D. dissertation concerned photoabsorption-induced disordering (PAID), a technique which allows one to shift permanently the band-gap in a semiconductor MQW structure by laser beam irradiation.

During his Ph.D. work, he spent 14 months in the Optoelectronic Group of the University of Glasgow, U.K., where he applied PAID to the fabrication of lasers and electroabsorption optical modulators on InP. Recently, he has been involved at the University of Palermo in the fabrication of thin film devices on 3-D substrates using laser-direct writing techniques.

A. Catrina Bryce joined the Department of Electronics and Electrical Engineering, University of Glasgow, Glasgow, Scotland, in 1985 as a Research Assistant in MBE. In 1987, she joined the optoelectronics group to work on nonlinear optical properties of GaInAs quantum-well structures at 1.5 m. Since then, her research work has included GaInAs–InP electrooptic modulators, quantum-well intermixing, particularly in 1.55-m and 980-nm material systems and lasers at both 980 nm and 1.55 m. In February 1993, she was appointed to the post of Research Technologist. Her main research interests are optoelectronic integration and short-pulse semicoductor lasers.

Richard M. De La Rue was born in Reading, U.K., in 1945. He received the B.Sc.(Eng.) Honors degree in electrical engineering from University College, London (UCL), U.K., the M.A.Sc. degree in electrical engineering from the University of Toronto, Canada, and the Ph.D. degree, also from UCL, in 1966, 1968, and 1972, respectively.

In 1971, he was appointed as Lecturer in the Department of Electronics and Electrical Engineering at the University of Glasgow, Glasgow, Scotland, becoming Senior Lecturer in 1982, Reader in 1985, and Professor of Optoelectronics in 1986. He spent a six-month period at Bell Labs, Murray Hill, NJ, in 1978 and three months as a Monbusho/British Council-sponsored Lecturer at Tohoku University, Sendai, Japan, in 1980. He has contributed significantly to integrated optics research in glass based waveguides, including the use of ion-exchange techniques. Such waveguides have been used in more recent research on optical waveguide molecular sensors. Work on lithium niobate led to the first publications in the U.K. on waveguide devices (both electrooptic and acoustooptic) and some of the earliest waveguide devices in the world based on proton-exchange in lithium niobate. He was involved in pioneering work on electron beam-induced domain reversal to produce periodic structures for quasi-phase-matched SHG. Other work has included fundamental studies of the proton-exchange process in lithium niobate and lithium tantalate. Recent work has been concerned primarily with integration technology and optoelectronic devices based on III-V semiconductor quantum-well heterostructures. Research has included quantum-well intermixing processes in III-V semiconductors to shift the refractive index and absorption edge and novel forms of DFB and DBR laser using deep surface gratings. He has also contributed to the development of ring-geometry semiconductor lasers, particularly large-diameter mode-locked devices. Following an extended period as leader of the SERC/EPSRC Rolling Grant-supported optoelectronics research activity at Glasgow University, he has now shifted a significant part of his research effort into the photonic bandgap structures/microcavities area. He has published more than 170 articles and papers in journals, book chapters, and conference presentations. He was co-editor, with John Marsh, of *Waveguide Optoelectronics*, based on the 1990 NATO ASI held in Glasgow.

John H. Marsh (M'91–SM'91) was born in Edinburgh, Scotland, in 1956. He received the B.A. degree in engineering and electrical sciences from the University of Cambridge, U.K., in 1977, the M.Eng. degree in solid state electronics from the University of Liverpool, U.K., in 1978, and the Ph.D. degree from Sheffield University, U.K., in 1982. His research at Sheffield University involved LPE growth and electrical transport properties of InGaAsP alloys.

He joined the Department of Electronics and Electrical Engineering at the University of Glasgow, Glasgow, Scotland, in 1986, where he is currently Professor of Optoelectronic Systems. His research interests are particularly concerned with linear and nonlinear integrated optoelectronic devices in III-V semiconductors. He has developed new integration technologies for photonic integrated circuits based on quantum-well devices and quantum-well intermixing. He is author or co-author of more than 200 journal and conference papers. He is a corresponding editor of the *IEE Electronics and Communication Journal*. He was Director of the NATO Advanced Study Institute on Waveguide Optoelectronics held in Glasgow in 1990 and is co-editor of the book with the same name. He is currently a member of the editorial board of the *International Journal of Optoelectronics* and Chair of the Scottish Chapter of LEOS.

Dr. Marsh is a Fellow of the Royal Society of Arts and a member of the Institution of Electrical Engineers (IEE) and of the British Association for Crystal Growth. He was a committee member of the IEE Professional Group concerned with Optical Devices and Systems from 1988 until 1994.

Christopher C. Button was born in Ipswich, Suffolk, U.K., in September 1957. He received the B.A. degree from the Open University, U.K., in 1988.

He joined the research laboratories of the Delta Metals Group in Ipswich in 1976 and studied chemistry to the LRIC level at Suffolk College. He then joined British Telecom Research Laboratories (BTRL) at Martlesham in 1981. He was sponsored by BTRL to study with the Open University. He has been employed at the EPSRC Central Facility for III-V Semiconductors at the University of Sheffield. U.K., since 1988, where he is a Research Fellow, responsible for the MOCVD growth of phosporus-containing compounds.